

Synthesis, Structure, Reactivity and Electrochemistry of *cis*-Dioxoruthenium-(vi) and -(v) Complexes containing *N,N,N',N',3,6*-Hexamethyl-3,6-diazaoctane-1,8-diamine†

Chi-Keung Li, Chi-Ming Che,* Wai-Fong Tong, Wai-Tong Tang, Kwok-Yin Wong and Ting-Fong Lai

Department of Chemistry, University of Hong Kong, Pokfulam Road, Hong Kong

The complexes *cis*-[Ru^{VI}LO₂]²⁺, *cis*-[Ru^VLO₂]⁺ and *cis*-[Ru^{III}L(MeCN)₂]²⁺ (L = *N,N,N',N',3,6*-hexamethyl-3,6-diazaoctane-1,8-diamine) have been prepared and their structures determined. The two Ru=O bonds in *cis*-[Ru^{VI}LO₂]²⁺ are equivalent [1.795(9) Å] and the O–Ru–O angle is 112.0(4)°. In *cis*-[Ru^VLO₂]⁺ the two Ru=O distances are 1.751(3) and 1.756(4) Å, and the O–Ru–O angle is 115.1(2)°. The N(MeCN)–Ru–N(MeCN) angle in *cis*-[Ru^{III}L(MeCN)₂]²⁺ is 86.1(2)°. The cyclic voltammogram of *cis*-[Ru^{VI}LO₂]²⁺ in acetonitrile exhibits a reversible one-electron Ru^{VI}–Ru^V couple at 0.53 V vs. Ag–AgNO₃ (0.1 mol dm⁻³). In aqueous solutions, proton-coupled electron-transfer redox couples are observed. This complex is capable of oxidising a wide variety of organic substrates including 2,3-dimethylbutane and adamantane. Oxidation of saturated alkanes occurred preferentially at the tertiary C–H bond.

The design of oxoruthenium compounds for selective oxidation of organic substrates is of current interest.¹ There are ample examples in the literature illustrating that monooxoruthenium-(vi) and -(v) and *trans*-dioxoruthenium(vi) complexes having different redox potentials can readily be prepared, some of which have been characterised by X-ray crystallography.¹ However, the oxidation chemistry of *cis*-dioxoruthenium-(vi) and -(v) remains unexplored. Although several reports have described the chemical and electrochemical generation of *cis*-dioxoruthenium-(v) and -(vi) complexes of aromatic diimines in aqueous solutions,^{2–4} difficulty has been encountered in the isolation of these classes of compounds because of their extreme reactivities.

For several years we have been working on the synthesis of high-valent oxoruthenium complexes of chelating tertiary amine ligands.⁵ We envisaged that the tetradentate tertiary amine L (*N,N,N',N',3,6*-hexamethyl-3,6-diazaoctane-1,8-diamine), because of its small cavity size upon co-ordination to a metal ion, would be a good ligand for the fabrication of ruthenium complexes having a *cis*-dioxo unit. In a previous report the synthesis of an oxoruthenium complex of L through oxidation with H₂O₂ was described.^{5c} This complex was unstable in aqueous solutions. We have modified the synthesis by using Ce^{IV} as the oxidant. Herein is described the structure, electrochemistry and reactivities of *cis*-dioxoruthenium-(vi) and -(v) complexes of L. Since the completion of this work an unusual *cis*-dioxoruthenium(vi) complex, *cis*-[RuO₂(MeCO₂)Cl₂]⁻, has been structurally characterised by Griffith *et al.*⁶

Experimental

Materials.—K₂[RuCl₅(H₂O)] (Johnson and Matthey) was used as received. Trifluoroacetic acid (99%, Aldrich) was purified by distillation under a nitrogen atmosphere. Acetonitrile (Mallinkrodt, Chrom AR) was purified by treatment with KMnO₄ and then distilled over CaH₂. Water was distilled twice from alkaline KMnO₄. Tetrabutylammonium fluoroborate (Southwestern Analytical Chemicals, Electrometric Grade) for electrochemical studies was dried in a vacuum oven at 100 °C

for 24 h. The organic substrates were purified by literature methods⁷ and the purity was checked by gas chromatography and ¹H NMR spectroscopy. The ligand L and the metal complex *cis*-[Ru^{III}LCl₂]⁺ClO₄⁻ were prepared according to published procedures.^{5c}

cis-[Ru^{VI}LO₂]²⁺[ClO₄]₂⁻. A mixture of *cis*-[Ru^{III}LCl₂]⁺ClO₄⁻ (0.3 g) and silver toluene-*p*-sulfonate (0.6 g) in distilled water (25 cm³) was heated to about 80 °C for 0.5 h. The resulting solution was filtered to remove the insoluble AgCl and was oxidised by an aqueous solution of [NH₄]₂[Ce(NO₃)₆] (2 g in 5 cm³) at room temperature. Green crystalline *cis*-[Ru^{VI}LO₂]²⁺[ClO₄]₂⁻ was slowly deposited upon addition of NaClO₄. The product could be recrystallised from 0.1 mol dm⁻³ HClO₄ (yield ≈ 70%) (Found: C, 29.0; H, 6.2; Cl, 14.2; N, 11.3. Calc.: C, 28.9; H, 6.0; Cl, 14.3; N, 11.2%). UV/VIS [λ_{\max} /nm (ϵ /dm³ mol⁻¹ cm⁻¹) in 0.1 mol dm⁻³ CF₃CO₂H]: 661 (42), 325 (1400) and 227 (5200).

cis-[Ru^{III}L(MeCN)₂]²⁺[ClO₄]₂⁻. The complex *cis*-[Ru^{VI}LO₂]²⁺[ClO₄]₂⁻ (0.1 g) was stirred with benzyl alcohol (1 cm³) or norbornene (1 g) in acetonitrile (20 cm³) for 5 h. Yellow solid *cis*-[Ru^{III}L(MeCN)₂]²⁺[ClO₄]₂⁻ was precipitated upon addition of diethyl ether. The crude product was recrystallised by vapour diffusion of diethyl ether into an acetonitrile solution. Yield nearly quantitative (Found: C, 31.5; H, 6.1; Cl, 11.5; N, 13.8. Calc.: C, 31.4; H, 5.9; Cl, 11.6; N, 13.7%). UV/VIS [λ_{\max} /nm (ϵ /dm³ mol⁻¹ cm⁻¹) in MeCN]: 379 (200) and 300 (250).

cis-[Ru^VLO₂]⁺ClO₄⁻. This complex was generated by constant-potential reduction of *cis*-[Ru^{VI}LO₂]²⁺ at 0.4 V vs. Ag–AgNO₃ (0.1 mol dm⁻³) in acetonitrile or by standing an acetonitrile solution of *cis*-[Ru^{VI}LO₂]²⁺[ClO₄]₂⁻ at room temperature for 24 h. μ_{eff} (Evans method): 1.9. UV/VIS [λ_{\max} /nm (ϵ /dm³ mol⁻¹ cm⁻¹) in MeCN]: 325 (1300).

cis-[Ru^{IV}L(O)(H₂O)]²⁺. This complex was generated by constant-potential reduction of *cis*-[Ru^{VI}LO₂]²⁺ at 0.70 V vs. saturated calomel electrode (SCE) in 0.1 mol dm⁻³ CF₃CO₂H. The complex was too soluble to be isolated. UV/VIS [λ_{\max} /nm (ϵ /dm³ mol⁻¹ cm⁻¹) in 0.1 mol dm⁻³ CF₃CO₂H]: 320 (850) and 510 (70).

X-Ray Structure Analysis.—X-Ray diffraction data for the ruthenium complexes were measured on an Enraf-Nonius CAD4 diffractometer with graphite-monochromated Mo-K α radiation by using the ω -2 θ scanning technique in the bisecting mode. The unit-cell dimensions were obtained from a least-

† Supplementary data available: see Instructions for Authors, *J. Chem. Soc., Dalton Trans.*, 1992, Issue 1, pp. xx–xxv.

squares fit of 25 well centred reflections. Intensity data were corrected for Lorentz, polarisation and absorption effects; the empirical absorption was based on azimuthal (ψ) scans of nine reflections with $80 < \psi < 90^\circ$. For *cis*-[Ru^{VI}LO₂][ClO₄]₂, the check reflections showed a drop in intensity of 12% at the end of data collection; correction for linear decay was also applied. Crystal and structure determination data are summarised in Table 1. Atomic scattering factors were taken from ref. 8. Calculations were carried out on a MicroVax II computer using the Enraf-Nonius SDP program.⁹

The structures were solved by Patterson and Fourier techniques and refined by full-matrix least squares. The refinement of *cis*-[Ru^VLO₂][ClO₄] and *cis*-[Ru^{III}L(MeCN)₂][ClO₄]₂ was straightforward. All the non-hydrogen atoms were refined anisotropically and the hydrogen atoms obtained either from Fourier difference maps (for those in the methyl groups) or by calculation at idealised positions (for those in the methylene groups) were allowed to ride on their attached carbon atoms with assigned isotropic thermal parameters. The oxygen atoms in the perchlorate ion of *cis*-[Ru^{III}L(MeCN)₂][ClO₄]₂, however, showed abnormally large thermal motion; each of these atoms was subsequently refined isotropically over two sites with occupancy factors of 0.5. Final agreement factors are given in Table 1.

The refinement of *cis*-[Ru^{VI}LO₂][ClO₄]₂ was somewhat complicated. From the systematic absences the space group could be either *Pn2₁a* or *Pnma*. Since there are only four formula units per unit cell and the cation does not possess a centre or mirror plane of symmetry the space group *Pn2₁a* was first assumed. The refinement showed however some unreasonable bond lengths and angles in the macrocycle and furthermore the coordinates of both the cation and anions gave strong indication of mirror symmetry with the mirror planes perpendicular to the *c* axis. The space group was then switched to *Pnma* with the assumption that the macrocycle was disordered. In the proposed model for the cation two enantiomorphs were superimposed so that the atoms Ru, N(1), N(3), C(1) and C(7)

which lie on a crystallographic mirror plane and atoms O(1), C(2), C(4), C(6) and C(8) together with their mirror images were common to both, whereas the disordered atoms N(2A), N(2B), C(3) and C(5) belonged to one and their mirror images N(2A'), N(2B'), C(3') and C(5') belonged to the other enantiomorph [See Fig. 1(a)]. During the final least-squares cycles the disordered atoms were refined isotropically and all other non-hydrogen atoms anisotropically; hydrogen atoms were omitted. The final agreement factors are given in Table 1.

Selected bond distances and angles and atomic coordinates of *cis*-[Ru^{VI}LO₂]²⁺, *cis*-[Ru^VLO₂]⁺ and *cis*-[Ru^{III}L(MeCN)₂]²⁺ are listed in Tables 2 and 3.

Additional material available from the Cambridge Crystallographic Data Centre comprises H-atom coordinates, thermal parameters and remaining bond lengths and angles.

Physical Measurements.—Elemental analyses of the complexes were performed by Butterworth Laboratories. Infrared spectra were measured in Nujol mull on a Nicolet 20SX FTIR spectrophotometer, electronic absorption spectra with a Shimadzu UV240 spectrophotometer. The magnetic susceptibilities of solid samples were measured at room temperature by the Guoy method using Hg[Co(SCN)₄]₂ as calibrant. For samples in solution the Evans method was employed.

Cyclic voltammetry was performed with a Princeton Applied Research (PAR) model 175 universal programmer and model 173 potentiostat. The working electrode was pyrolytic graphite or glassy carbon. Controlled-potential coulometry was performed using a PAR model 377A coulometric cell and a model 179 digital coulometer.

Stoichiometric oxidation of organic substrates was performed by dissolving the complex *cis*-[Ru^{VI}LO₂][ClO₄]₂ (0.05 mmol) and the organic substrate (0.5 mmol) in acetonitrile (1 cm³). The reaction mixture was stirred with a magnetic stirrer under nitrogen at room temperature. A control experiment in the absence of the ruthenium complex was performed for each

Table 1 Crystal parameters and experimental data *

Molecular formula	<i>cis</i> -[Ru ^{VI} LO ₂][ClO ₄] ₂	<i>cis</i> -[Ru ^V LO ₂][ClO ₄]	<i>cis</i> -[Ru ^{III} L(MeCN) ₂][ClO ₄] ₂
<i>M</i>	562.37	462.92	612.48
Space group	<i>Pnma</i> (no. 62)	<i>P2₁/c</i> (no. 14)	<i>I2/a</i> (non-standard form of no. 15)
Crystal system	Orthorhombic	Monoclinic	Monoclinic
<i>a</i> /Å	13.272(2)	12.858(3)	15.499(2)
<i>b</i> /Å	9.386(2)	9.563(2)	10.358(1)
<i>c</i> /Å	17.372(2)	15.694(4)	15.671(2)
β /°		105.43(2)	93.99(1)
<i>U</i> /Å ³	2164	1860.0	2509.5
<i>Z</i>	4	4	4
<i>F</i> (000)	1152	956	1264
<i>D_c</i> /g cm ⁻³	1.726	1.653	1.621
μ (Mo-K α)/cm ⁻¹	10.1	10.0	8.8
<i>T</i> /K	293 \pm 1	294 \pm 1	294 \pm 1
Crystal dimensions/mm	0.10 \times 0.22 \times 0.38	0.46 \times 0.25 \times 0.18	0.06 \times 0.10 \times 0.26
Scan speed/° min ⁻¹	0.8–5.5	0.66–5.49	1.0–5.5
Collection range	2 θ _{max} = 50°; $\pm h, k, l$	2 θ _{max} = 55°; $\pm h, k, \pm l$	2 θ _{max} = 50°; $\pm h, \pm k, l$
Scan width/°	0.80 \pm 0.34tan θ	0.60 \pm 0.34tan θ	1.00 \pm 0.34tan θ
Background time	25% of full scan width on both sides	0.5 \times scan time	25% of full scan width on both sides
Reflections measured	4185	5703	4790
Independent reflections	2195	4533	2332
Reflections used in calculations	1219	3456	1555
[<i>I</i> > 1.5 σ (<i>I</i>)], <i>m</i>			
Parameters refined, <i>p</i>	124	217	146
<i>R</i>	0.074	0.058	0.059
<i>R'</i>	0.101	0.072	0.075
<i>S</i>	2.75	1.62	1.96
Residual electron density in ΔF map/ e Å ⁻³	+1.34, -0.97	2.15, -1.58	0.86, -0.63

* Weighting scheme: $w = 4F_o^2/[\sigma^2(F_o^2) + (pF_o^2)^2]$

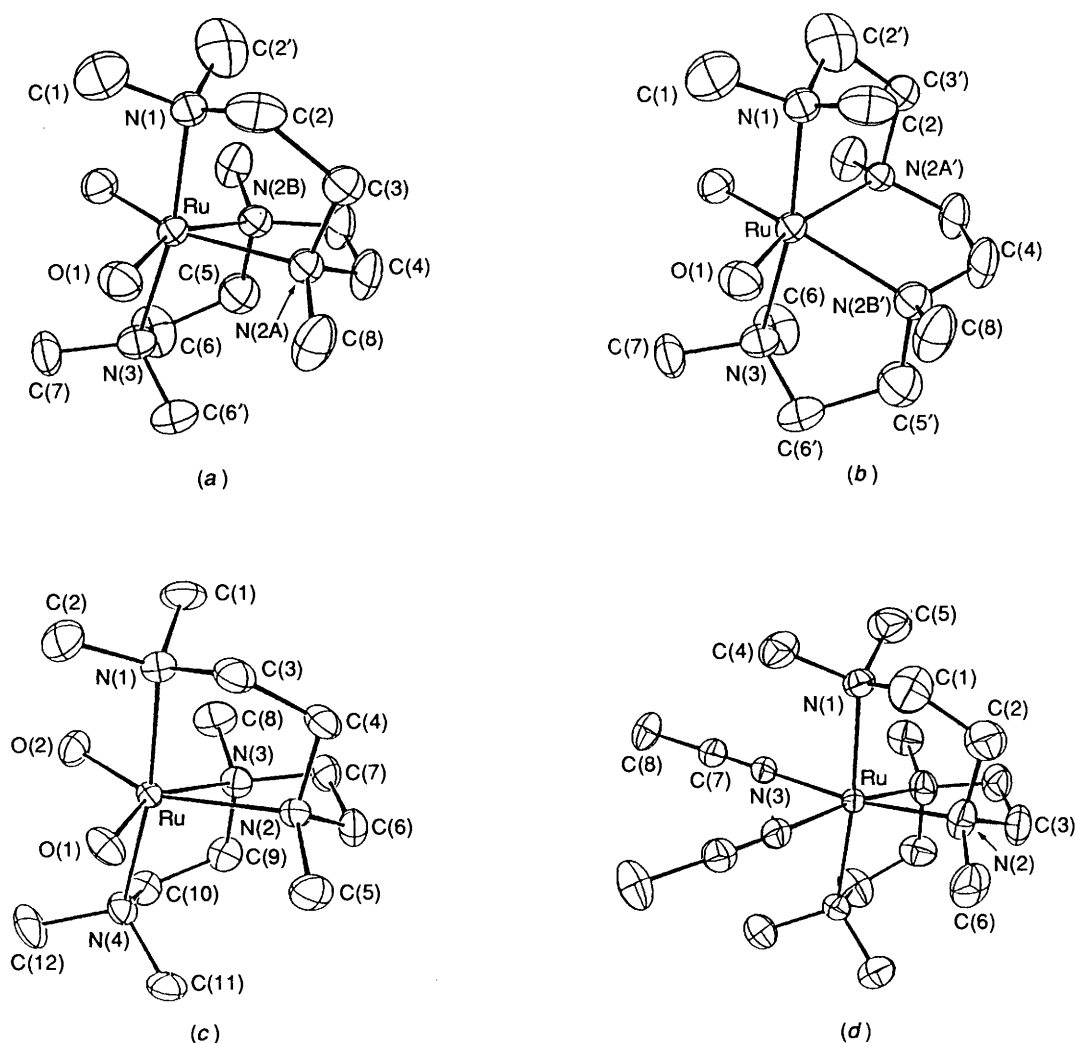


Fig. 1 The ORTEP plots of the two enantiomorphs of *cis*-[Ru^{VI}LO₂]²⁺ (a) and (b), of *cis*-[Ru^VLO₂]⁺ (c) and of *cis*-[Ru^{II}L(MeCN)₂]²⁺ (d). The thermal ellipsoids are drawn at the 35% probability level

reaction. The products were analysed by gas chromatography, ¹H NMR, mass and UV/VIS spectroscopy. Gas chromatographic analyses were conducted using a Varian model 940 gas chromatograph equipped with a flame ionisation detector and a 6 ft column containing 10% (w/w) Carbowax 20 M on Chromosorb W. Individual gas chromatographic components were quantitated by the internal standard method employing a Shimadzu C-R3A electronic integrator.

Results and Discussion

In a previous report the synthesis and X-ray structure of *cis*-[Ru^{III}LCl₂]⁺ were described.^{5c} Treatment of *cis*-[Ru^{III}LCl₂]⁺ with Ag^I followed by oxidation with H₂O₂ at 60 °C gave an oxoruthenium complex which was assigned as *trans*-[Ru^{VI}LO₂]²⁺ based on IR spectroscopy. However, this complex was unstable in aqueous solution at pH > 3; the mechanism of degradation is not yet known. However, recent studies indicated that under certain conditions the complex *cis*-[Os^{VI}LO₂]²⁺ would undergo intra-ligand rearrangement to give *cis*-[Os^{VI}L'(NMe₃)O₂]²⁺ (L' = 1,4,7-trimethyl-1,4,7-triazacyclononane)¹⁰ whose structure has been characterised by X-ray crystallography.

In the present study, the oxidant H₂O₂ was replaced by Ce^{IV} and the oxidation was carried out at room temperature. The green complex *cis*-[Ru^{VI}LO₂][ClO₄]₂ prepared in this way is stable in the solid state for several days and in aqueous solution

for about 3 h. In highly purified acetonitrile it is stable for about 2 h at room temperature, but is slowly reduced by the solvent to *cis*-[Ru^VLO₂]⁺ and finally to *cis*-[Ru^{II}L(MeCN)₂]²⁺ upon prolonged standing. As expected for d² *cis*-dioxometal complexes,^{6,11-13} *cis*-[Ru^{VI}LO₂][ClO₄]₂ is diamagnetic and shows two intense IR bands at 874 and 859 cm⁻¹ with different intensity, tentatively assigned to the symmetric and asymmetric Ru=O stretches. Attempts have been made to prepare *cis*-[Ru^{VI}L(¹⁸O)₂]²⁺ through exchange with H₂¹⁸O. However, no ¹⁸O was incorporated into the metal complex at room temperature. The extreme reactivity of *cis*-[Ru^{VI}LO₂]²⁺ precludes any labelling study at temperatures higher than 50 °C. The existence of two Ru=O stretches is in accord with a *cis* geometry, which has also been confirmed by X-ray crystallography. Previous work showed that *trans*-dioxoruthenium(vi) complexes of neutral amines show a characteristic (d_{xy})² → (d_{xy})¹(d_π^{*})¹ (d_π^{*} = d_{xy}, d_{yz}) absorption band with ν(Ru=O) vibrational progression at 380–400 nm.^{5a,14} The present *cis*-dioxoruthenium(vi) complex does not show such a band at room temperature. Instead an intense band with ε_{max} of 1400 dm³ mol⁻¹ cm⁻¹ appears at 325 nm, which is likely due to a ligand (N or O)-to-metal (Ru) charge-transfer transition. There is a low-energy absorption band at 662 nm, which is absent for the *trans*-dioxoruthenium(vi) system. The low ε_{max} of this band suggests that it is due to the transition(s) within the d orbitals.

Unlike previous work where *cis*-dioxoruthenium(v) was only observed as a transient intermediate during cyclic voltammetric

scans in aqueous solutions,⁴ $cis-[Ru^V LO_2]^+$ has been generated by electrochemical and chemical reduction of $cis-[Ru^{VI} LO_2]^{2+}$ in acetonitrile. The measured μ_{eff} of 1.9 for $cis-[Ru^V LO_2]ClO_4$ is in accordance with a low-spin d^3 electronic configuration for oxoruthenium(V). It is stable in acetonitrile for several hours and could be reoxidised back to the starting Ru^{VI} . Its UV/VIS spectrum is featureless, being dominated by the high-energy $p_n(O) \rightarrow d_n(Ru)$ charge-transfer transition at 325 nm. Only one of the two $\nu(Ru=O)$ stretches in $cis-[Ru^V LO_2]ClO_4$ could be located at 850 cm^{-1} ; the remaining one probably overlaps with the ligand stretching modes.

Structures of $cis-[Ru^{VI} LO_2][ClO_4]_2$, $cis-[Ru^V LO_2]ClO_4$ and $cis-[Ru^{II} L(MeCN)_2][ClO_4]_2$.—Fig. 1(a)–(c) shows ORTEP

Table 2 Selected bond distances (Å) and angles (°)

<i>(a) $cis-[Ru^{VI} LO_2]^{2+}$</i>			
Ru–O(1)	1.795(9)	N(2A)–C(8)	1.49(2)
Ru–N(1)	2.17(1)	N(2B)–C(4) ^a	1.44(2)
Ru–N(2A)	2.22(2)	N(2B)–C(5)	1.56(4)
Ru–N(2B)	2.25(3)	N(2B)–C(8) ^a	1.49(3)
Ru–N(3)	2.20(1)	N(3)–C(6)	1.45(3)
N(1)–C(1)	1.42(3)	N(3)–C(7)	1.49(2)
N(1)–C(2)	1.48(2)	C(2)–C(3)	1.69(3)
N(2A)–C(3)	1.54(3)	C(4)–C(4) ^a	1.51(3)
N(2A)–C(4)	1.45(2)	C(5)–C(6)	1.67(4)
O(1)–Ru–O(1) ^a	112.0(4)	O(1)–Ru–N(1)	89.7(3)
O(1)–Ru–N(2A)	86.8(6)	O(1) ^a –Ru–N(2A)	160.4(6)
O(1)–Ru–N(2B)	157.3(7)	O(1) ^a –Ru–N(2B)	85.9(7)
O(1)–Ru–N(3)	84.9(3)	N(1)–Ru–N(2A)	84.9(5)
N(1)–Ru–N(2B)	104.7(6)	N(1)–Ru–N(3)	170.3(5)
N(2A)–Ru–N(2B)	77.4(7)	N(2A)–Ru–N(3)	102.8(5)
N(2B)–Ru–N(3)	83.0(6)		
<i>(b) $cis-[Ru^V LO_2]^+$</i>			
Ru–O(1)	1.751(3)	N(2)–C(6)	1.474(7)
Ru–O(2)	1.756(4)	N(3)–C(7)	1.487(6)
Ru–N(1)	2.155(4)	N(3)–C(8)	1.475(7)
Ru–N(2)	2.296(4)	N(3)–C(9)	1.490(7)
Ru–N(3)	2.316(4)	N(4)–C(10)	1.471(8)
Ru–N(4)	2.163(4)	N(4)–C(11)	1.465(7)
N(1)–C(1)	1.477(6)	N(4)–C(12)	1.502(6)
N(1)–C(2)	1.491(8)	C(3)–C(4)	1.493(8)
N(1)–C(3)	1.490(7)	C(6)–C(7)	1.498(8)
N(2)–C(4)	1.498(7)	C(9)–C(10)	1.508(8)
N(2)–C(5)	1.483(7)		
O(1)–Ru–O(2)	115.1(2)	O(2)–Ru–N(4)	87.3(2)
O(1)–Ru–N(1)	86.7(2)	N(1)–Ru–N(2)	80.8(1)
O(1)–Ru–N(2)	86.1(1)	N(1)–Ru–N(3)	106.6(1)
O(1)–Ru–N(3)	155.3(2)	N(1)–Ru–N(4)	171.6(1)
O(1)–Ru–N(4)	88.5(2)	N(2)–Ru–N(3)	75.8(1)
O(2)–Ru–N(1)	88.6(2)	N(2)–Ru–N(4)	105.8(1)
O(2)–Ru–N(2)	155.7(1)	N(3)–Ru–N(4)	80.4(1)
O(2)–Ru–N(3)	86.6(2)		
<i>(c) $cis-[Ru^{II} L(MeCN)_2]^{2+}$</i>			
Ru–N(1)	2.212(6)	N(2)–C(3)	1.45(1)
Ru–N(2)	2.148(8)	N(2)–C(6)	1.47(1)
Ru–N(3)	2.038(8)	N(3)–C(7)	1.14(1)
N(1)–C(1)	1.49(1)	N(3)···N(3) ^b	2.78(1) ^c
N(1)–C(4)	1.51(1)	C(1)–C(2)	1.47(2)
N(1)–C(5)	1.45(1)	C(3)–C(3) ^b	1.60(1)
N(2)–C(2)	1.56(1)	C(7)–C(8)	1.45(1)
N(1)–Ru–N(1)	174.3(3)	N(2)–Ru–N(3)	96.4(3)
N(1)–Ru–N(2)	84.0(3)	N(3)–Ru–N(3)	86.1(2)
N(1)–Ru–N(3)	88.1(3)	Ru–N(3)–C(7)	169.2(8)
N(2)–Ru–N(3)	171.6(3)	N(3)–C(7)–C(8)	177(1)
N(2)–Ru–N(2)	82.2(3)		

^a Symmetry code: $x, \frac{1}{2} - y, z$. ^b Symmetry code: $\frac{3}{2} - x, y, -z$. ^c Non-bonding distance.

plots of the $cis-[Ru^{VI} LO_2]^{2+}$ and $cis-[Ru^V LO_2]^+$ cations with the atom numbering. The structures feature the first examples of six-co-ordinated *cis*-dioxoruthenium-(VI) and -(V) complexes. In both complexes, the co-ordination geometry about the ruthenium atom is distorted octahedral with two Ru=O moieties *cis* to each other and the conformation adopted by ligand L is similar to that found in $cis-[Ru^{III} LCl_2]^+$.^{5c} The Ru–N(tertiary amine) distances are in the normal range expected for oxoruthenium complexes of tertiary amines.^{5a}

Perhaps the most interesting structural features are the Ru=O distances and O–Ru–O angles. The O–Ru–O angles, 112.0(4) and 115.1(2)° for Ru^{VI} and Ru^V respectively, are perhaps the smallest values reported for six-co-ordinated d^2 *cis*-dioxometal complexes. They are lower than those of 120.2(6)° in $cis-[RuO_2(MeCO_2)Cl_2]^-$,⁶ 127° in $[RuO_2Cl_3]^-$,¹¹ 121.4(4)° in $cis-[Re(bipy)(py)_2O_2]^+$ (bipy = 2,2'-bipyridine, py = pyridine),¹² and 127° in $cis-[OsO_2(MeCO_2)_3]^-$.¹³ The two Ru=O bonds in either $cis-[Ru^{VI} LO_2]^{2+}$ or $cis-[Ru^V LO_2]^+$ are equivalent. Except for $trans-[Ru^{IV}(py)_4O(Cl)]^+$,¹⁵ the measured Ru=O distance of 1.795(9) Å in $cis-[Ru^{VI} LO_2]^{2+}$ is perhaps the longest ever reported for Ru=O complexes. It is about 0.09 Å longer than that for its *trans* analogue $trans-[Ru^{VI}(16-tmc)O_2]^{2+}$ (16-tmc = 1,5,9,13-tetramethyl-1,5,9,13-tetraazacyclohexadecane)¹⁶ and $cis-[RuO_2(MeCO_2)Cl_2]^-$ (average Ru=O 1.685 Å).⁶ Interestingly, the Ru=O distances of 1.751–1.756 Å in $cis-[Ru^V LO_2]^+$ are even shorter than that in $cis-[Ru^{VI} LO_2]^{2+}$. Presumably, the larger O–Ru–O angle in $cis-[Ru^V LO_2]^+$ than in $cis-[Ru^{VI} LO_2]^{2+}$ helps to reduce the coulombic repulsive interaction of the two *cis*-oxo groups leading to a stronger metal–oxo bond. The Ru=O distances in ruthenium(V) complexes are greatly affected by the auxiliary ligands ranging from 1.687(6) Å in $[NPr_4][RuO(O_2)COC(OC_2)_2]^{17}$ 1.733(6) Å in $[RuO(CH_2SiMe_3)_3]^{18}$ 1.725(3) Å in $[L_{OEt}(O)Ru(O)Ru(O)O_{OEt}]\{L_{OEt} = (\eta-C_5H_5)Co[(EtO)_2P=O]_3\}^{19}$ to 1.751–1.756 Å in the present system. The present structural data clearly indicate that the Ru=O and Ru–N distances in $cis-[Ru^{VI} LO_2]^{2+}$ and $cis-[Ru^V LO_2]^+$ are similar, despite the change in the electronic configuration. This would mean a small inner-sphere reorganisation energy required for the reduction of *cis*-dioxoruthenium(VI) to *cis*-dioxoruthenium(V). Table 4 compares the Ru=O distances for various oxoruthenium(VI) complexes.

Fig. 1(d) shows an ORTEP plot of the $cis-[Ru^{II} L(MeCN)_2]^{2+}$ cation with atom numbering. The co-ordination geometry and conformation of L is virtually identical to that found in $cis-[Ru^{VI} LO_2]^{2+}$. Interestingly, the measured N(MeCN)–Ru–N(MeCN) angle of 86.1(2)° is significantly smaller than the Cl–Ru–Cl angle of 97.7° in the isostructural $cis-[Ru^{III} LCl_2]^+$.^{5c} Whether this arises from the constraint of the ligand L or the interaction of the two *cis*-MeCN molecules is uncertain.

Electrochemistry.—The cyclic voltammogram of $cis-[Ru^{VI} LO_2]^{2+}$ in acetonitrile (Fig. 2) shows a reversible one-electron

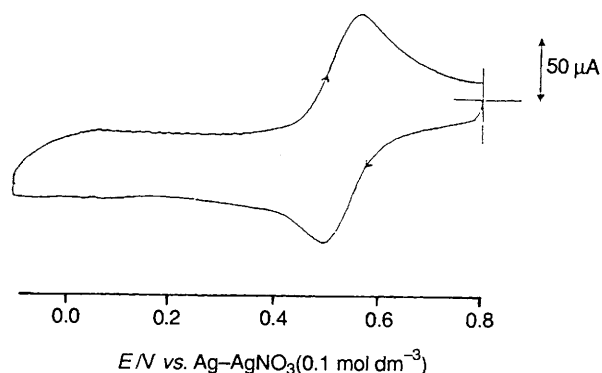


Fig. 2 Cyclic voltammogram of $cis-[Ru^{VI} LO_2]^{2+}$ in acetonitrile. Working electrode: edge-plane pyrolytic graphite. Scan rate: 100 mV s^{-1} . Supporting electrolyte: $0.1\text{ mol dm}^{-3} [NBu_4]BF_4$

Table 3 Atomic coordinates for non-hydrogen atoms with estimated standard deviations in parentheses

(a) <i>cis</i> -[Ru ^{VI} LO ₂][ClO ₄] ₂				(b) <i>cis</i> -[Ru ^V LO ₂]ClO ₄			
Atom	x	y	z	Atom	x	y	z
Ru	0.191 8(1)	0.250	0.039 12(8)	N(2A) ^a	0.275(1)	0.392(2)	0.119(1)
Cl(1)	0.539 6(4)	0.250	0.733 1(3)	N(2B) ^a	0.224(1)	0.106(2)	0.140(1)
Cl(2)	0.668 2(4)	0.250	0.104 6(3)	N(3)	0.039(1)	0.250	0.087 9(9)
O(1)	0.151 9(6)	0.409(1)	-0.009 9(5)	C(1)	0.306(2)	0.250	-0.107(1)
O(11)	0.455(2)	0.250	0.691(1)	C(2)	0.389(1)	0.381(2)	-0.012(1)
O(12)	0.544(3)	0.250	-0.194(2)	C(3) ^a	0.381(2)	0.412(3)	0.084(1)
O(13)	0.597(2)	0.365(2)	0.713(1)	C(4)	0.292(1)	0.331(2)	0.194 2(7)
O(21)	0.645(1)	0.250	0.024(1)	C(5) ^a	0.123(2)	0.098(4)	0.185(2)
O(22)	0.588(2)	0.250	0.145(1)	C(6)	0.019(1)	0.122(2)	0.133(1)
O(23)	0.732(1)	0.133(2)	0.122 8(8)	C(7)	-0.035(1)	0.250	0.023(1)
N(1)	0.329 6(9)	0.250	-0.027 6(8)	C(8)	0.244(1)	0.545(2)	0.120 8(9)
(c) [Ru ^{III} L(MeCN) ₂][ClO ₄] ₂ ^b				(d) [Ru ^{III} L(O)(H ₂ O)] ₂ ⁺			
Ru	0.750	0.037 54(9)	0.000	C(7)	0.843 3(6)	-0.197 7(9)	-0.083 5(5)
Cl	0.406 4(1)	0.458 0(2)	0.169 4(1)	C(8)	0.874 8(7)	-0.317 0(9)	-0.116 9(7)
N(1)	0.654 6(4)	0.026 9(7)	-0.111 5(4)	O(11)	0.396(1)	0.592(2)	0.187(1)
N(2)	0.670 4(5)	0.193 8(7)	0.038 8(5)	O(12)	0.430 5(9)	0.374(2)	0.233(1)
N(3)	0.817 2(4)	-0.106 3(7)	-0.054 4(4)	O(13)	0.455(1)	0.435(2)	0.099(1)
C(1)	0.575 2(7)	0.086(1)	-0.080 4(8)	O(14)	0.322(1)	0.452(2)	0.137(1)
C(2)	0.596 1(7)	0.205(1)	-0.033 7(8)	O(21)	0.333(2)	0.416(3)	0.212(2)
C(3)	0.717 4(7)	0.315 1(9)	0.037 6(7)	O(22)	0.442 0(9)	0.584(1)	0.198 2(9)
C(4)	0.631 0(7)	-0.110(1)	-0.137 3(7)	O(23)	0.377(1)	0.428(2)	0.089(1)
C(5)	0.677 8(8)	0.090(1)	-0.189 6(6)	O(24)	0.472(1)	0.382(2)	0.189(1)
C(6)	0.623 9(7)	0.180(1)	0.116 9(6)				

^a Occupancy factor = 0.50. ^b Occupancy factor for O atoms in perchlorate group = 0.5.

Table 4 The Ru=O bond distances of some oxoruthenium(vi) complexes

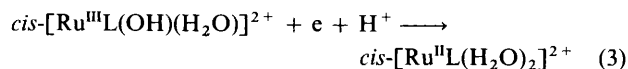
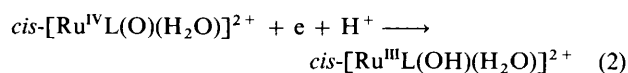
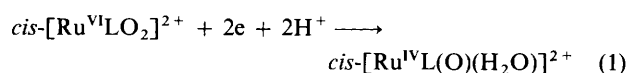
Complex	Ru=O/Å	Ref.
<i>trans</i> -[Ru(15-tmc)O ₂] ²⁺ ^a	1.718(5)	16
<i>trans</i> -[Ru(16-tmc)O ₂] ²⁺	1.705(7)	16
<i>trans</i> -[Ru(bipy)O ₂ (MeCO ₂) ₂]	1.726(1)	20
<i>trans</i> -[Ru(terpy)O ₂ (H ₂ O)] ²⁺ ^b	1.661	21
<i>trans</i> -[RuO ₂ (HIO ₆) ₂] ⁶⁻	1.732(8)	22
[RuO ₃ (OH) ₂] ²⁻	1.763(2), 1.760(2), 1.741(2)	23
<i>trans</i> -[RuO ₂ Cl ₄] ²⁻	1.709(4)	11
[Ru ₂ O ₆ (py) ₄]	1.73(1)	24
<i>cis</i> -[RuO ₂ (MeCO ₂)Cl ₂] ⁻	1.64, 1.71	6
<i>cis</i> -[RuLO ₂] ²⁺	1.795(9)	This work

^a 15-tmc = 1,4,9,12-Tetramethyl-1,5,9,12-tetraazacyclopentadecane.

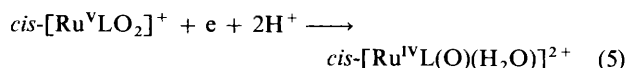
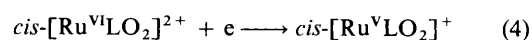
^b terpy = 2,2': 6', 2''-Terpyridine.

couple at 0.53 V *vs.* Ag-AgNO₃ (0.1 mol dm⁻³). Constant-potential coulometry established *n* = 1.0, suggesting a Ru^{VI}-Ru^V couple. In aqueous solutions, proton-coupled electron-transfer redox couples are observed. Fig. 3 shows the cyclic voltammograms at different pH. At pH 1.0 two reversible couples I and III at 0.80 and 0.26 V respectively and one ill defined couple II at 0.63 V (*vs.* SCE) were found. Constant-

potential coulometry established the respective *n* values to be 1.9, 1.0 and 1.0, suggesting the electrode reactions (1)-(3). At



pH 2.0 couple I starts to split into two reversible one-electron couples IV and V, appearing at 0.77 and 0.71 V respectively. These are assigned as the Ru^{VI}-Ru^V and Ru^V-Ru^{IV} couples (4) and (5). At pH 4.5 couples II and V merge to form a new couple



VI. The relative magnitudes of the peak currents for couples IV, VI and III are in the ratio 1:2:1. Constant-potential coulometry established that couple VI corresponds to the two-electron reduction of Ru^V to Ru^{III}, equation (6).

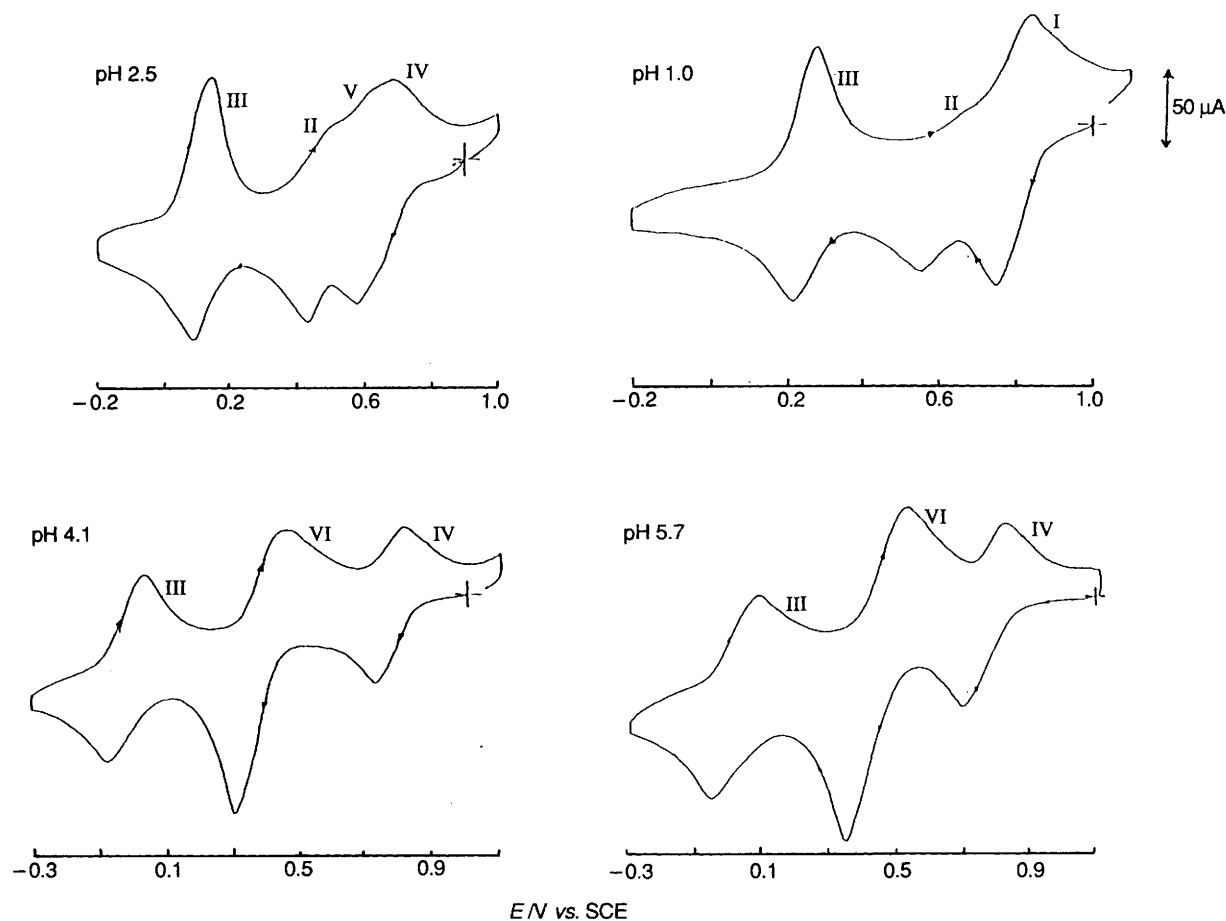
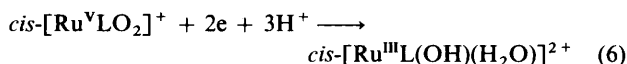
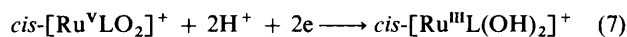


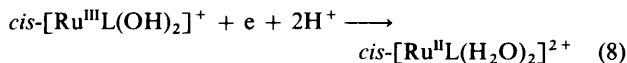
Fig. 3 Cyclic voltammograms of $\text{cis-}[\text{Ru}^{\text{VI}}\text{LO}_2]^{2+}$ at different pH. Working electrode and scan rate as in Fig. 2



When the pH of the medium is raised the E° of all redox couples, except that of IV, shift cathodically. The Pourbaix diagram over the range pH 1–11 is shown in Fig. 4. Linear plots of E° versus pH with slopes close to -60 and -118 mV per pH unit are found for couples I and V respectively, in accordance with their formulations. For couple VI there are two straight-line fragments with slopes of -90 and -57 mV per pH unit at $4.5 < \text{pH} < 6.5$ and at $\text{pH} > 6.5$ respectively. On the basis of these findings, the corresponding electrode reactions are (6) and (7). For couple III the slope of the plot is -60 mV per pH unit at



$1 < \text{pH} < 6.5$ but becomes -117 mV per pH unit at $\text{pH} > 6.5$. Thus the corresponding electrode reactions are (3) and (8). The



break point of the plot for couple III occurs at pH 6.5, which is logically the pK_a value of $\text{cis-}[\text{Ru}^{\text{III}}\text{L}(\text{OH})(\text{H}_2\text{O})]^{2+}$.

Oxidation of Organic Substrates.—Table 5 summarises the result of stoichiometric oxidation of organic substrates by $\text{cis-}[\text{Ru}^{\text{VI}}\text{LO}_2]^{2+}$ in acetonitrile at room temperature. Control experiments showed negligible oxidation in the absence of the ruthenium oxidant. However, even in acetonitrile only, some of the complex was converted into $\text{cis-}[\text{Ru}^{\text{II}}\text{L}(\text{MeCN})_2]^{2+}$ after 4 h. This may explain the low percentage yields (Table 5) found in some of the oxidation reactions investigated. For each of the

stoichiometric oxidations studied after 4 h the ruthenium product isolated through precipitation with diethyl ether was $\text{cis-}[\text{Ru}^{\text{II}}\text{L}(\text{MeCN})_2]^{2+}$, suggesting that either two oxygen atoms were used in the oxidation or the intermediate $\text{cis-}[\text{Ru}^{\text{IV}}\text{L}(\text{O})(\text{H}_2\text{O})]^{2+}$ was unstable and disproportionated in acetonitrile.

Alcohols were rapidly oxidised to the corresponding aldehydes/ketones in a two-step reaction. When the reaction was followed by UV/VIS spectroscopy a species having a similar optical spectrum to that of $\text{cis-}[\text{Ru}^{\text{IV}}\text{L}(\text{O})(\text{H}_2\text{O})]^{2+}$ was formed within 1 h and gradually transformed to $\text{cis-}[\text{Ru}^{\text{II}}\text{L}(\text{MeCN})_2]^{2+}$ after several hours. Attempts to isolate the intermediate species in pure form were unsuccessful since some $\text{cis-}[\text{Ru}^{\text{II}}\text{L}(\text{MeCN})_2][\text{ClO}_4]_2$ was always found. For the reactions with alkenes the spectral changes were similar. Product analyses revealed that both epoxides and carbonyl products were formed. Attempts to detect the diol product by ^1H NMR spectroscopy were unsuccessful. Oxidation of cyclohexene gave cyclohex-2-en-1-one and cyclohex-2-en-1-ol with no cyclohexene oxide. This result is consistent with previous work which showed that $\text{Ru}=\text{O}$ complexes have a high affinity towards oxidation of allylic C–H bonds. The reaction with *cis*-stilbene gave a mixture of *cis*- and *trans*-stilbene oxides together with benzaldehyde. The loss of stereospecificity in the *cis*-stilbene oxidation according to Castellino and Bruce²⁵ is an indication of a charge-transfer mechanism.

Aromatic hydrocarbons were oxidised to the corresponding aldehydes/ketones. Since the oxidation of ethylbenzene and cumene gave the respective acetophenone and phenylpropan-2-ol, the relative reactivities of the C–H bonds follow the order: tertiary > secondary > primary. Interestingly, saturated alkanes such as adamantane and 2,3-dimethylbutane could also be oxidised at room temperature, indicating that oxidation

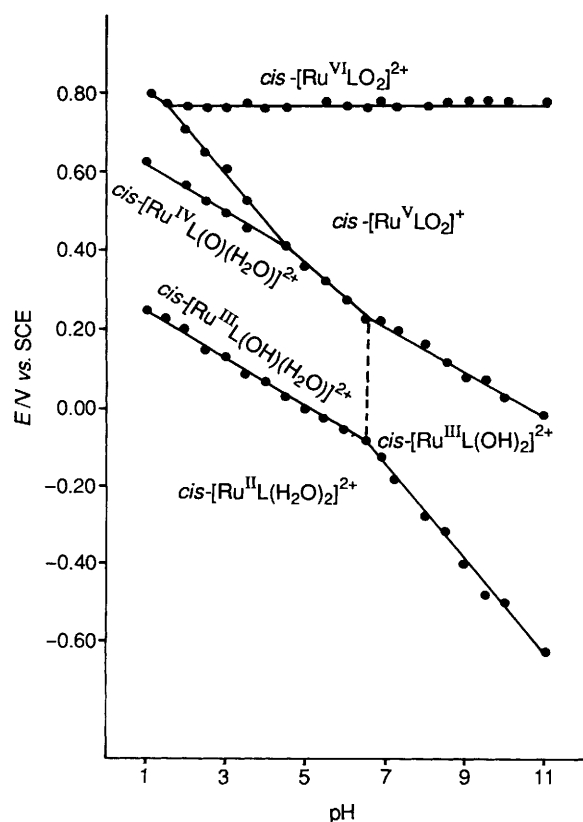


Fig. 4 Pourbaix plot for all redox couples of $cis-[Ru^{VI}LO_2]^{2+}$

Table 5 Results of stoichiometric oxidation of organic substrates by $cis-[Ru^{IV}LO_2]^{2+}$ in acetonitrile at 25 °C

Substrate	Product	Yield (%) [*]
Cyclohexanol	Cyclohexanone	86
Cyclopentanol	Cyclopentanone	70
Cyclobutanol	Cyclobutanone	74
Styrene	Styrene oxide	5
	Benzaldehyde	60
<i>cis</i> -Stilbene	<i>cis</i> -Stilbene oxide	30
	<i>trans</i> -Stilbene oxide	12
	Benzaldehyde	30
<i>trans</i> -Stilbene	<i>trans</i> -Stilbene oxide	15
	Benzaldehyde	32
Cyclohexene	Cyclohex-2-en-1-one	45
	Cyclohex-2-en-1-ol	20
Norbornene	<i>exo</i> -2,3-Epoxynorbornane	30
Cyclooctene	Cyclooctene oxide	55
Toluene	Benzaldehyde	45
Ethylbenzene	Acetophenone	58
	<i>sec</i> -phenethyl alcohol	17
Cumene	2-Phenylpropan-2-ol	56
Adamantane	Adamantan-1-ol	34
2,3-Dimethylbutane	2,3-Dimethylbutan-2-ol	13

* Based on amount of complex used.

occurred preferentially at the tertiary C–H bond. No reaction with cyclohexane was observed.

General Comments.—There have been few reports on d^2 *cis*-dioxometal complexes.⁸ Reported examples of this class of complexes include the structurally characterised $cis-[Re^V(bipy)(py)_2O_2]^+$ ¹² and $cis-[Os^{VI}(MeCO_2)_3O_2]^-$,¹³ neither of which is reactive towards organic oxidation. With the exception of *cis*-

$[Ru^{VI}(dcby)O_2]^{2+}$ (*dcby* = 6,6'-dichloro-2,2'-bipyridine)³ and $cis-[Ru^{VI}(dmphen)_2O_2]^{2+}$ (*dmphen* = 2,9-dimethyl-1,10-phenanthroline),² most of the reported *cis*-dioxometal complexes are not capable of oxidising alkenes and alkanes under mild conditions.¹⁰ However, the extreme reactivities of *cis*-dioxoruthenium(vi) complexes of aromatic diimines render studies on their reactions in solution difficult. In a recent molecular orbital calculation by Cundari and Drago²⁶ *cis*-dioxoruthenium(vi) was suggested to be much more reactive than its *trans* counterpart. These workers also suggested that the monooxoruthenium(-iv) and (-v) and *trans*-dioxoruthenium(vi) can only participate in concerted [2 + 2] or non-concerted [1 + 2] cycloaddition with alkenes, whereas *cis*-dioxoruthenium(vi) could also react *via* a concerted [3 + 2] cycloaddition pathway.²⁶ The [3 + 2] pathway has also been suggested by Corey *et al.*²⁷ to be responsible for alkene dihydroxylation.

In the present work, $cis-[Ru^{VI}LO_2]^{2+}$ and $cis-[Ru^{V}LO_2]^+$ have been generated and characterised. The lowering in the E^0 value of about 400 mV from $cis-[Ru^{VI}(bipy)_2O_2]^{2+}$ ($E^0 = 1.23$ V *vs.* SCE at pH 1)^{4b,c} to $cis-[Ru^{VI}LO_2]^{2+}$ is in agreement with previous findings that chelating tertiary amines are useful ligands for the stabilisation of high-valent oxoruthenium complexes.⁵ The characterisation of $cis-[Ru^{V}LO_2]^+$, $cis-[Ru^{IV}L(O)(H_2O)]^{2+}$ and $cis-[Ru^{II}L(MeCN)_2]^{2+}$ from the redox reactions of $cis-[Ru^{VI}LO_2]^{2+}$ suggests that *cis*-dioxoruthenium(vi) can function as an overall one-, two- or four-electron oxidant.

It is interesting to compare $trans-[Ru^{VI}(14-tmc)O_2]^{2+}$ ^{5a} (14-tmc = 1,4,8,11-tetramethyl-1,4,8,11-tetraazacyclotetradecane) and $cis-[Ru^{VI}LO_2]^{2+}$ since both complexes contain a chelating tetradentate tertiary amine ligand. The much longer Ru=O bond distances (1.71 *vs.* 1.795 Å) and the higher E^0 value (0.67 *vs.* 0.80 V at pH 1.0) for the latter complex suggest that with the same auxiliary ligand *cis*-dioxoruthenium(vi) should be a better oxidant. This is also reflected in the results of stoichiometric oxidation. While $cis-[Ru^{VI}LO_2]^{2+}$ is capable of oxidising a wide variety of organic substrates, $trans-[Ru^{VI}(14-tmc)O_2]^{2+}$ is not capable of oxidising alkenes and aromatic hydrocarbons under the same reaction conditions.^{5a}

One may expect *cis*-dioxoruthenium(vi) to behave differently from other known monooxo- and *trans*-dioxo-ruthenium complexes, especially in reactions with alkenes. In its reaction with styrene and *cis*- and *trans*-stilbene $cis-[Ru^{VI}LO_2]^{2+}$ behaves similarly to other monooxometal complexes such as those of Cr^V.^{28,29} Furthermore its reactions with a number of alkenes did not give the corresponding diol products; instead, as with other Ru=O species, the carbonyl products resulting from oxidative C=C bond cleavage and epoxides were obtained.^{3a,5b,30–32} These findings favour a non-concerted [1 + 2] cycloaddition pathway, involving electrophilic attack of a Ru=O moiety on the olefinic double bond. However, Cundari and Drago²⁶ also noted that a [3 + 2] cycloaddition of *cis*-dioxoruthenium(vi) with alkene would give the dioxometallacycle intermediate which easily rearranges leading to the C=C bond cleavage. In fact a large amount of carbonyl product was observed in the reaction of styrene with $cis-[Ru^{VI}LO_2]^{2+}$ (Table 5).

Acknowledgements

We acknowledge support from the Hong Kong Research Grants Council and the University of Hong Kong. C.-K. Li is the recipient of a fellowship, administered by the Sir Edward Youde Foundation.

References

- 1 W. P. Griffith, *Transition Met. Chem.*, 1990, **15**, 251.
- 2 C. L. Bailey and R. S. Drago, *J. Chem. Soc., Chem. Commun.*, 1987, 179; A. S. Goldstein and R. S. Drago, *J. Chem. Soc., Chem. Commun.*, 1992, 21.

- 3 (a) C. M. Che and W. H. Leung, *J. Chem. Soc., Chem. Commun.*, 1987, 1376; (b) C. M. Che and W. O. Lee, *J. Chem. Soc., Chem. Commun.*, 1988, 881.
- 4 (a) K. J. Takeuchi, G. J. Samuels, S. W. Gersten, J. A. Gilbert and T. J. Meyer, *Inorg. Chem.*, 1983, **22**, 1407; (b) J. C. Dobson and T. J. Meyer, *Inorg. Chem.*, 1988, **27**, 3283; (c) C. M. Che, K. Y. Wong, W. O. Lee and F. C. Anson, *J. Electroanal. Chem. Interfacial Electrochem.*, 1991, **309**, 303; (d) J. P. Collin and J. P. Sauvage, *Inorg. Chem.*, 1986, **25**, 135.
- 5 (a) C. M. Che, T. F. Lai and K. Y. Wong, *Inorg. Chem.*, 1987, **26**, 2289; (b) C. M. Che, W. T. Tang, W. T. Wong and T. F. Lai, *J. Am. Chem. Soc.*, 1989, **111**, 9048; (c) C. M. Che, W. T. Tang, H. W. Lam and T. C. W. Mak, *J. Chem. Soc., Dalton Trans.*, 1988, 2885; (d) C. M. Che, W. T. Tang, W. O. Lee, W. T. Wong and T. F. Lai, *J. Chem. Soc., Dalton Trans.*, 1989, 2011; (e) C. M. Che, W. T. Tang and C. K. Li, *J. Chem. Soc., Dalton Trans.*, 1990, 3735.
- 6 W. P. Griffith, J. M. Jolliffe, S. V. Ley and D. J. Williams, *J. Chem. Soc., Chem. Commun.*, 1990, 1219.
- 7 D. D. Perrin and W. L. F. Armarego, *Purification of Laboratory Chemicals*, 3rd edn., Pergamon, Oxford, 1988, ch. 3.
- 8 *International Tables for X-Ray Crystallography*, Kynoch Press, Birmingham, 1974, vol. 4, pp. 72, 149.
- 9 SDP Structure Determination Package, Enraf-Nonius, Delft, 1985.
- 10 C. M. Che, W. Y. Yu, T. C. W. Mak and Y. Wang, unpublished work.
- 11 S. Perrier and J. K. Kochi, *Inorg. Chem.*, 1988, **27**, 4165.
- 12 R. L. Blackburn, L. M. Jones, M. S. Ram, M. Sabat and J. T. Hupp, *Inorg. Chem.*, 1990, **29**, 1791.
- 13 T. Behling, M. V. Capparelli, A. C. Skapski and G. Wilkinson, *Polyhedron*, 1982, **1**, 840.
- 14 C. M. Che, K. Y. Wong, W. H. Leung and C. K. Poon, *Inorg. Chem.*, 1986, **25**, 345.
- 15 Y. Yukawa, K. Aoyagi, M. Kurihara, K. Shirai, K. Shimizu, M. Mukaida, T. Takeuchi and H. Kakihana, *Chem. Lett.*, 1985, 283.
- 16 T. C. W. Mak, C. M. Che and K. Y. Wong, *J. Chem. Soc., Chem. Commun.*, 1985, 986.
- 17 A. C. Dengel, W. P. Griffith, C. A. O'Mahoney and D. J. Williams, *J. Chem. Soc., Chem. Commun.*, 1989, 1720.
- 18 R. P. Tooze, G. Wilkinson, M. Motevalli and M. B. Hursthouse, *J. Chem. Soc., Dalton Trans.*, 1986, 2711.
- 19 J. M. Power, K. Evertz, L. Henling, R. Marsh, W. P. Schaefer, J. A. Labinger and J. E. Bercaw, *Inorg. Chem.*, 1990, **29**, 5058.
- 20 T. C. Lau and J. K. Kochi, *J. Chem. Soc., Chem. Commun.*, 1987, 798.
- 21 A. Dovletoglou, S. A. Adeyemi, M. H. Lynn, D. J. Hodgson and T. J. Meyer, *J. Am. Chem. Soc.*, 1990, **112**, 8989.
- 22 A. M. El-Hendawy, W. P. Griffith, B. Piggott and D. J. Williams, *J. Chem. Soc., Dalton Trans.*, 1988, 1983.
- 23 M. O. Elout, W. G. Haije and W. J. A. Naaskant, *Inorg. Chem.*, 1988, **27**, 610.
- 24 A. C. Dengel, A. M. El-Hendawy, W. P. Griffith, C. A. O'Mahoney and D. J. Williams, *J. Chem. Soc., Dalton Trans.*, 1990, 737.
- 25 A. J. Castellino and T. C. Bruice, *J. Am. Chem. Soc.*, 1988, **110**, 158; T. C. Bruice, *Aldrichim. Acta*, 1988, **21**, 87.
- 26 T. R. Cundari and R. S. Drago, *Inorg. Chem.*, 1990, **29**, 2303.
- 27 E. J. Corey, P. D. Jardine, S. Virgil, P. W. Yuen and R. D. Connell, *J. Am. Chem. Soc.*, 1989, **111**, 9243.
- 28 E. G. Samsel, K. Srinivasan and J. K. Kochi, *J. Am. Chem. Soc.*, 1985, **107**, 7606.
- 29 J. M. Garrison, D. Ostovic and T. C. Bruice, *J. Am. Chem. Soc.*, 1989, **111**, 4960.
- 30 C. Ho, C. M. Che and T. C. Lau, *J. Chem. Soc., Dalton Trans.*, 1990, 967; M. E. Marmion, R. A. Leising and K. J. Takeuchi, *J. Coord. Chem.*, 1988, **19**, 1; M. E. Marmion and K. J. Takeuchi, *J. Am. Chem. Soc.*, 1988, **110**, 1472.
- 31 J. T. Groves and R. Quinn, *J. Am. Chem. Soc.*, 1985, **107**, 5790.
- 32 J. C. Dobson, W. K. Seok and T. J. Meyer, *Inorg. Chem.*, 1986, **25**, 1514.

Received 15th November 1991; Paper 1/05802I